

# LLaVA-PruMerge: Adaptive Token Reduction for Efficient Large Multimodal Models

Yuzhang Shang<sup>1,2,\*</sup> Mu Cai<sup>1,\*</sup> Bingxin Xu<sup>2</sup> Yong Jae Lee<sup>1,†</sup> Yan Yan<sup>2,†</sup>

<sup>1</sup>University of Wisconsin–Madison <sup>2</sup>Illinois Institute of Technology

<https://lava-prumerge.github.io>

## Abstract

Large Multimodal Models (LMMs) have shown significant reasoning capabilities by connecting a visual encoder and a large language model. LMMs typically use a fixed amount of visual tokens, such as the penultimate layer features in the CLIP visual encoder, as the prefix content. Recent LMMs incorporate more complex visual inputs, such as high-resolution images and videos, which increase the number of visual tokens significantly. However, due to the design of the Transformer architecture, computational costs associated with these models tend to increase quadratically with the number of input tokens. To tackle this problem, we explore a token reduction mechanism and find, similar to prior work, that many visual tokens are spatially redundant. Based on this, we propose PruMerge, a novel adaptive visual token reduction approach, which largely reduces the number of visual tokens while maintaining comparable model performance. We first select the unpruned visual tokens based on their similarity to class tokens and spatial tokens. We then cluster the pruned tokens based on key similarity and merge the clustered tokens with the unpruned tokens to supplement their information. Empirically, when applied to LLaVA-1.5 [Liu et al., 2023a], our approach can compress the visual tokens by **18 times** on average, and achieve comparable performance across diverse visual question-answering and reasoning tasks.

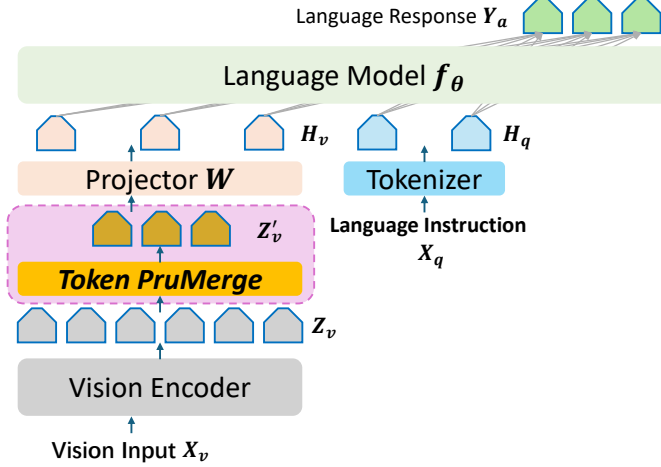
## 1 Introduction

Large Language Models (LLMs) [OpenAI, 2023b, Team et al., 2023, Jiang et al., 2023, Touvron et al., 2023] have shown strong reasoning abilities. LLMs are usually high-capacity Transformers pretrained with a large-scale text corpus. Large Multimodal Models (LMMs), inherit the LLMs for text generation, but also leverage a visual encoder such as CLIP-ViT [Radford et al., 2021] to embed image patches into visual tokens as the prefix visual context.

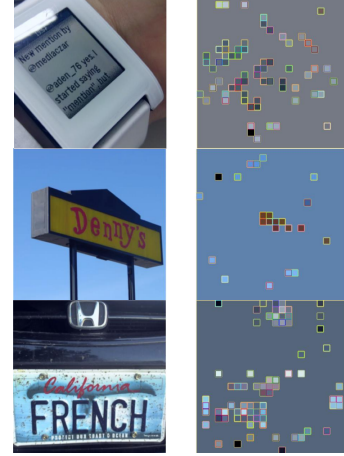
LMMs need substantial computation to conduct inference. The LLM is the primary factor for the high computation cost, since the visual encoder is usually quite small relative to the LLM. For example, the commonly used CLIP visual encoder, ViT-L, only has 0.3B parameters, while the corresponding LLM such as LLaMA [Touvron et al., 2023] or Vicuna [Vicuna, 2023] can have 7B or 13B parameters. As a result, reducing the LLM’s inference cost is the key to achieving low LMM inference cost.

Prior works [Chu et al., 2023, 2024, Yuan et al., 2023a] mainly focus on replacing the LLM backbone with a smaller language model with less parameters, such as Phi-2 [Javaheripi et al., 2023]. However, such approaches sacrifice the reasoning abilities of LLMs, leading to a large performance gap in visual question-answering and reasoning such as VQAv2 and MM-Bench [Chu et al., 2024]. A similar approach is to apply quantization for LLMs [Liu et al., 2023b, Yuan et al., 2024].

\*Equal Contribution. † Equal Advising Author. Work done during Yuzhang’s visit to UW-Madison.



(a) Main idea of **LLaVA-PruMerge**.



(b) PruMerged Token Visualization.

Figure 1: **(a)** We prune and merge the visual tokens coming from the vision encoder, while keeping all other procedures of the LMM the same. By reducing the number of visual tokens, our proposed method, PruMerge, significantly reduces the computation cost for text generation in LMMs. **(b)** The visualizations of the attentive tokens. We design a token reduction method to **adaptively** select visual tokens based on the information density of the visual input, enabling the LLM to perceive visual input effectively and efficiently. More attentive tokens are sampled in complex images such as ones with text, while fewer are sampled on simpler images. Besides, such attentive tokens are usually located at the regions with dense information.

However, the cost of LLMs comes from not only its large number of parameters, but also the length of the input context due to the quadratic complexity of the Transformer’s attention operation. The context length in LMMs is especially important, where a fixed amount of visual tokens serves as the prefixed tokens. For example, in LLaVA-1.5, 576 visual tokens are appended, leading to high training and inference costs. Thus, an intriguing question is: *Can we reduce the number of prefix visual tokens while maintaining comparable performance?*

In our study, we find that such visual tokens are redundant, similar to findings in previous related work Bolya et al. [2023], Liu et al. [2022], and most of the visual tokens can be pruned without largely sacrificing the performance. In particular, we find that the activations are very sparse upon the similarity matrix between the class token and spatial patches, which indicates that only a small amount of the visual tokens are related to the key visual information in the image. Motivated by this, we use this similarity to select important visual tokens. Specifically, we leverage the Interquartile Range (IQR) [Boukerche et al., 2020] scoring function in outlier detection to prune the visual tokens. Moreover, we merge the visual tokens using  $k$ -nearest neighbor and update the sampled visual tokens via weighted averaging, which further enhances performance. Finally, we optionally finetune the LLM to let the model better adapt to our token deduction design.

Empirically, PruMerge can effectively and adaptively reduce the visual tokens in each image in LLaVA-1.5 [Liu et al., 2023a], where with just 5.5% of visual tokens, which is around 32 tokens on average, LLaVA-PruMerge can maintain comparable performance with that of retaining all 576 tokens across diverse benchmarks. Our work demonstrates the effectiveness of building efficient LMMs from the perspective of visual token reduction and paves the road for further research.

## 2 Related Work

### 2.1 Efficient Large Multimodal Models (LMMs)

Large Language Models (LLMs) such as GPT-4 [OpenAI, 2023b], LLaMA [Touvron et al., 2023], Mistral [Jiang et al., 2023], and Gemini [Team et al., 2023] have demonstrated strong question answering and reasoning capabilities over text. Large Multimodal Models (LMMs) [Liu et al., 2023b, Zhu et al., 2023, Yin et al., 2023, Zhang et al., 2024] extend these reasoning capabilities to images, where given an image and an associated question, a vision encoder and an LLM are leveraged to

generate text responses in a chat format. More recent works extend whole-image understanding into region-level understanding [Cai et al., 2024, Zhang et al., 2023b, Peng et al., 2023, Chen et al., 2023], video understanding [Lin et al., 2023, Zhang et al., 2023a] and 3D scene understanding [Hong et al., 2023]. Such works typically feed the visual tokens directly into the LLM as prefix tokens, via either MLP [Liu et al., 2023a], Qformer [Dai et al., 2023, Zhu et al., 2023], or resampler [Alayrac et al., 2022]. The number of visual tokens can be prohibitively long, especially when the images are high-resolution [Liu et al., 2024, OpenAI, 2023a]. In this paper, we reduce the number of visual tokens by leveraging the similarity between the class token and the spatial patch tokens.

The need for cross-modal capabilities in resource-limited scenarios has become increasingly important. Despite advancements in LMMs, their large-scale training and deployment incur significant computational costs, necessitating efficient parallel device implementations. Google’s Gemini [Team et al., 2023] is a leader in efficient LMMs, achieving state-of-the-art performance on multimodal benchmarks and introducing mobile-scale LMMs suitable for low-memory devices. However, Gemini remains closed-source. Open-source initiatives, like LLaVA-1.5 [Liu et al., 2023a], utilize advanced compression techniques, such as 4/8 bit quantization [Dettmers et al., 2022, Shang et al., 2024]. Further efforts towards efficient LMMs include MobileVLM [Chu et al., 2023], which develops a compact LLM and an efficient multimodal feature projector, and its successor, MobileVLM-v2 [Chu et al., 2024], which explores improved training strategies for mobile scenarios. TinyGPT-V [Yuan et al., 2023a] leverages the advanced Phi-2 [Javaheripi et al., 2023] LLM to surpass the performance of significantly larger models. Similarly, LLaVA-Phi [Zhu et al., 2024] and Vary-toy [Wei et al., 2024] introduce smaller backbones and enhanced vocabularies for broader generalizability. TinyLLaVA [Zhou et al., 2024] investigates the impacts of architectural choices, data quality, and training strategies, demonstrating that smaller LMMs can match the performance of their larger counterparts with optimized data and training. MoE-LLaVA [Lin et al., 2024] adapts Mixture of Experts (MoE) to mitigate model degradation due to sparsity.

In most cases, LMM efficiency is enhanced by reducing the size of the backbone of the LMM, but no work has considered the efficiency of the LMM from the perspective of the number of visual tokens.

## 2.2 Token Reduction

The notorious squared complexity in Transformers [Vaswani et al., 2017] is a well-known problem, as it is one of the key bottlenecks in scaling the sequence length. Sparse attention such as Linformer [Wang et al., 2020] and ReFormer [Kitaev et al., 2020] reduce the quadratic attention complexity by conducting attention operations within a certain region rather than the full context. Token merging [Bolya et al., 2023] utilizes full attention but gradually reduces the number of tokens in each transformer block by selecting the most representative tokens with bipartite matching. In recent LMMs [Liu et al., 2023b, Zhu et al., 2023], prefix visual tokens serve as a fixed budget for context, which becomes one of the leading factors for their efficiency. In our study, we find that by simply pruning and merging visual tokens based on their similarity, we can achieve comparable performance using less than one tenth of the original tokens.

## 3 Method: Token Pru-Merging

In this section, we first review the basic implementation of large multimodal models (LMMs), with a particular focus on the visual encoder component (*i.e.*, Vision Transformer). We highlight the direct correlation between the number of visual tokens and the efficiency of LMMs (Sec. 3.1). Next, we present a plug-and-play token reduction method specifically designed for LMMs, called token PruMerge. Our method features two key components: (1) Adaptive Important Token Selection (AITS) via Outlier Detection which adaptively determines the optimal number of visual tokens to retain based on the unique characteristics of the image (Sec. 3.2); and (2) Token Supplement (TS) via Similar Key Clustering, which facilitates more efficient processing without compromising the model’s performance by maintaining the integrity and richness of the visual information (Sec. 3.3).

### 3.1 Preliminaries

**Vision Transformers (ViTs)** [Dosovitskiy et al., 2020] are the most widely used vision encoder for large multimodal models, in which the input image is converted into a sequence of representative

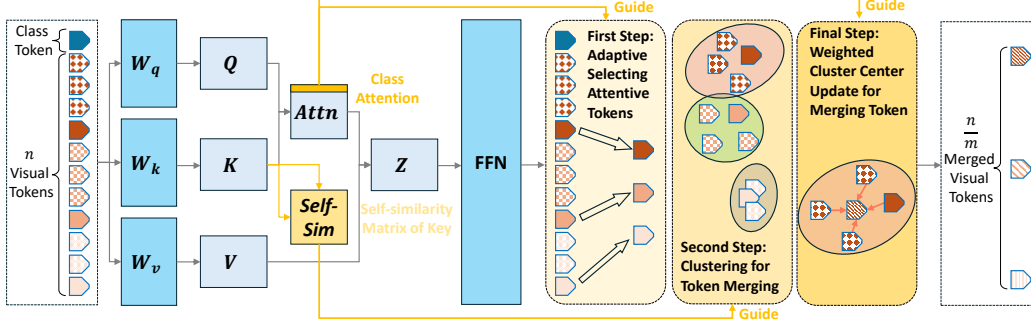


Figure 2: The conceptual idea of LLaVA-PruMerge. Our approach has 3 steps: (1) Sample important tokens according to the similarities between the class tokens and spatial visual tokens; (2) Cluster the visual tokens via  $k$ -nearest neighbor; and (3) Adjust the sampled visual tokens via weighted averaging for each cluster. Here  $m$  denotes the visual token compression ratio.

tokens by the ViT, and then feed into an LLM for understanding [Liu et al., 2024, Zhu et al., 2023, Hong et al., 2023, Zhang et al., 2024]. ViTs perform tokenization by dividing an input image into patches and projecting each patch into a token embedding. An extra class token [CLS] is added to the set of image tokens and is responsible for aggregating global image information and performing classification. Let  $n$  denote the number of input tokens (image patches) to the ViT. ViTs are composed of a series of transformer blocks. An assembly of several key components composes each transformer block: a multi-head self-attention layer, a feed-forward neural network (FFN), shortcut connections, and layer normalization [Ba et al., 2016], all of which work together to enhance the model’s ability to capture and interpret visual information [Han et al., 2022]. In the **self-attention layer**, an input token is projected into three distinct vectors: the query vector  $\mathbf{q}$ , the key vector  $\mathbf{k}$ , and the value vector  $\mathbf{v}$ , utilizing three linear transformation matrices  $\mathbf{W}_q$ ,  $\mathbf{W}_k$ , and  $\mathbf{W}_v$ . These vectors, corresponding to different inputs, are assembled into matrices  $\mathbf{Q}$ ,  $\mathbf{K}$ , and  $\mathbf{V}$ . The self-attention mechanism computes the relevance of each item to other items as follows:

$$\mathbf{Y} = \text{Self-Attention}(\mathbf{Q}, \mathbf{K}, \mathbf{V}) = \mathbf{A} \cdot \mathbf{V} \quad (3.1)$$

where attention matrix  $\mathbf{A} = \text{softmax}\left(\frac{\mathbf{Q} \cdot \mathbf{K}^T}{\sqrt{d_k}}\right)$  and  $d_k$  represents the dimension of  $\mathbf{q}$ ,  $\mathbf{k}$ ,  $\mathbf{v}$ . In the last encoder layer of ViT, the [CLS] token is used for classification. Similarly, the attention between [CLS] token and other visual tokens are performed via the attention mechanism:

$$\mathbf{a}_{\text{cls}} = \text{softmax}\left(\frac{\mathbf{q}_{\text{cls}} \cdot \mathbf{K}^T}{\sqrt{d_k}}\right). \quad (3.2)$$

The multi-head self-attention framework allows for simultaneous focus on multiple positions, offering diverse representation subspaces. This is achieved by employing distinct query, key, and value matrices for different heads, which project the input vectors into varied representation subspaces. Subsequent to the self-attention layers is the feed-forward network (FFN). This network consists of two linear transformation layers separated by a nonlinear activation function and is represented as:

$$\text{FFN}(\mathbf{X}) = \mathbf{W}_2 \sigma(\mathbf{W}_1 \mathbf{X}) \quad (3.3)$$

with  $\mathbf{W}_1$  and  $\mathbf{W}_2$  being the parameter matrices of the linear transformation layers and  $\sigma$  denoting the nonlinear activation function, such as GELU [Hendrycks & Gimpel, 2016]. The general forward pass of ViT is illustrated in the left part of Figure 2.

**Large Multimodal Models (LMMs).** Following the forward pass through a Vision Transformer (ViT), a series of visual tokens is generated. These tokens are then processed by the input projector  $\Theta_{\mathbf{X} \rightarrow \mathbf{T}}$ , which is responsible for mapping the encoded features from other modalities  $\mathbf{F}_X$  into the text feature space  $\mathbf{T}$ . The aligned features and the text prompts  $\mathbf{P}_T$  are then fed into the LLM backbone [Zhang et al., 2024]. The overall architecture of LMMs is depicted in Figure 1. It is important to note that the computational cost associated with these models tends to increase quadratically with the number of input tokens fed into the LLM backbone [Tay et al., 2022]. There is an increasing demand for the processing of high-resolution images and videos, which increases the number of visual tokens, further exacerbating computation costs. The reduction of visual tokens presents a promising approach to improving the efficiency of LMMs by reducing the escalating computational requirements.

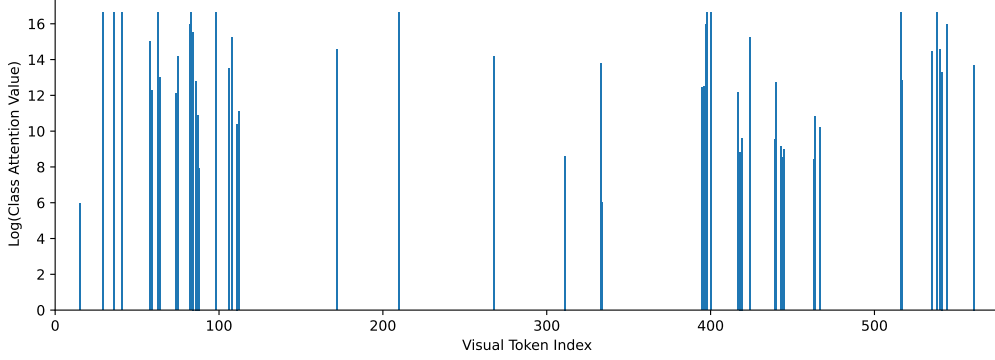


Figure 3: The distribution of attention values (in the penultimate layer of CLIP-ViT) between the `[cls]` token and visual tokens. The values in the y-axis are logarithmic values. Notably, most of the spatial visual tokens have near-zero attention values with the class token.

### 3.2 Adaptive Important Token Selection via Outlier Detection

The most straight-forward solution to improve the efficiency of visual token utilization in LMMs is to prune the redundant visual tokens [Liu et al., 2022, Yin et al., 2022, Liang et al., 2022]. To realize token pruning, we need to address a pivotal question: *How do we determine the importance of each visual token?*

As discussed in Sec. 3.1, LMMs typically leverage an extensive stack of visual tokens to represent the visual information. On the other hand, self-/weakly-supervised learning paradigms, such as CLIP [Radford et al., 2021] simplify this complexity by representing an entire image with a single `[cls]` token, regarded as the most information-condensed token. To balance those two extreme paradigms, we investigate the Key-Query attention between `[cls]` token and visual tokens, *i.e.*,  $a_{cls}$  in Equation 3.2. Observing the distribution patterns of attention between the `[cls]` token and visual tokens unveils a sparse landscape, as depicted in Figure 3. This sparse distribution underpins our methodology for identifying crucial visual tokens. By employing outlier detection algorithms, we aim to adaptively select visual tokens that best represent an image’s features effectively.

**Interquartile Range (IQR) Method for outlier detection.** To identify outliers within class attention values, we adopt the Interquartile Range (IQR) method [Boukerche et al., 2020], a statistical technique known for its robustness in outlier detection. The essence of the IQR method lies in its capability to establish a boundary or “fence” that delineates the normal range of data. This is achieved by calculating the IQR (the difference between the third quartile  $Q3$  and the first quartile  $Q1$ ) and subsequently defining the outer limits of the normal range as 1.5 times the IQR above  $Q3$  and below  $Q1$ . Specifically, the computation is as follows: the “lower fence” is set at  $1.5 \times \text{IQR}$  below  $Q1$ , and the “upper fence” is set at  $1.5 \times \text{IQR}$  above  $Q3$ . Any attention values residing outside these fences are classified as outliers. Through this method, we can adaptively identify and select the visual tokens for each image that exhibit outlier attention values, *i.e.*, those playing a significant role in representing the image within the LMM context. Note that we use the class attention value from the penultimate layer for this calculation.

As shown in Figure 1b, the sampled visual tokens demonstrate two behaviors: (1) The number of attentive tokens are proportional to the complexity of the image. Simpler images such as “*Billboard among blue sky*” owns fewer tokens while images with rich information such as a screen with dense texts own more tokens. (2) The sampled tokens are spatially aligned with the important details, while less tokens are assigned for the background. Such visualizations align with our visual token sampling design. These trends are also observed at the benchmark level. In Table 3, the average token numbers on various benchmarks differ.

### 3.3 Token Supplement via Similar Key Clustering

Following the selection of more informative visual tokens, we next optimize the utilization of the remaining tokens. While pruned tokens may initially seem extraneous, they hold potential value for the perception capabilities of the LLM backbone. This potential arises particularly in cases where an image contains large object parts that dominate the scene. In such scenarios, overly aggressive pruning could inadvertently diminish the model’s ability to represent the image comprehensively.



---

**Algorithm 1** Token PruMerge algorithm for reducing the number of visual tokens.

---

**Require:** Key and Query matrices of ViT’s penultimate layer,  $\mathbf{K} = \{\mathbf{k}_1, \dots, \mathbf{k}_n\}$  and  $\mathbf{Q} = \{\mathbf{q}_1, \dots, \mathbf{q}_n\}$ . The penultimate layer’s output tokens,  $\mathbf{Y} = \{\mathbf{y}_1, \dots, \mathbf{y}_n\}$ .  $n$  is the number of input visual tokens.

**Ensure:** Refine  $\mathbf{Y}$  to  $m$  (adaptive) visual token  $\mathbf{Y}' = \{\mathbf{y}'_1, \dots, \mathbf{y}'_m\}$ , in which  $m \ll n$ .

- 1: **Token PruMerge:**
  - 2: Calculate attention between visual token and class token  $\mathbf{a}_{[cls]}$  using Equation 3.2.
  - 3: Use the outlier detection algorithm IQR to **adaptively** select  $m$  important visual tokens’ index  $\{i_1, \dots, i_m\}$  based on  $\mathbf{a}_{[cls]}$  (see Sec. 3.2).
  - 4: **for**  $p = \{i_1, \dots, i_m\}$  **do**
  - 5:     Calculate the distance between selected token  $\mathbf{y}_p$  and other visual tokens,  $\mathbf{y}_{\{1, \dots, n\}/p}$ ;
  - 6:     Use  $\mathbf{y}_p$  as cluster center and run  $k$ -nearest neighbor algorithm to find  $k$  similar tokens, with indices  $\{j_1, \dots, j_k\}_p$ ;
  - 7:     Update cluster center token with weighted sum:  $\mathbf{y}'_p = \sum_{q=1}^k \mathbf{a}[j_q] \cdot \mathbf{y}_{j_q}$ ;
  - 8: **end for**
  - 9: (see Sec. 3.3).
  - 10: Output a refined stack of visual token  $\mathbf{Y}' = \{\mathbf{y}'_1, \dots, \mathbf{y}'_m\}$ .
- 

To address this, we devise a token merging method aimed at enhancing the representational capacity of the selected unpruned tokens. This method involves the strategic fusion of currently pruned tokens, as depicted in Figure 2. To choose the pruned tokens to merge, we need a way to measure similarity between visual tokens. Luckily, transformers natively solve this problem with QKV self-attention. Specifically, the keys ( $\mathbf{K}$ ) already summarize the information contained in each token for use in dot product similarity. Thus, we use a dot product similarity metric (e.g., cosine similarity) between the keys of each token to determine which tokens contain similar visual information [Bolya et al., 2023]. Specifically, the similarity between visual tokens is computed as

$$\text{Sim}(\mathbf{y}_i, \mathbf{y}_j) = \mathbf{k}_i \cdot \mathbf{k}_j^T, \quad (3.4)$$

which yields  $\mathbf{K}\mathbf{K}^T(i, j)$  for tokens  $i, j$  in vectorization form for the set of all tokens  $1, 2, \dots, n$ .

With the similarities between visual tokens established, we simply find the  $k$ -nearest neighbors for each unpruned token, which act as the cluster centers. The integration of pruned tokens into these clusters is guided by their respective class attentions  $\mathbf{a}[i]$ , enabling a refined representation of each unpruned token through a weighted sum. This procedure is outlined in Algorithm 1.

### 3.4 Discussion

**Distinction from Existing Token Reduction Methods.** Token reduction methods are especially proposed for inferring vision transformers (ViT) efficiently. Block by block, tokens are gradually reduced in number, correspondingly reducing the computation cost in the internal ViT. However, our approach work is not dedigned for efficient ViT, yet it serves as a plug-and-play module after the final outputs of visual encoder (*i.e.*, ViT). There are two benefits of this design. Firstly, while ViTs typically rely on a single class token to represent the input image, enabling them to maintain performance despite a reduction in intermediate tokens, LMMs usually leverage a large stack of visual tokens. This ensures a comprehensive representation of the visual content, preserving the model’s ability to capture nuanced details. Secondly, considering that the bulk of computational demand within LMMs is attributed to the LLM component rather than the ViT, our approach focuses not on the reduction of tokens but on maximizing the informational content of the pruned visual tokens. This strategy addresses the computational challenges inherent in LMMs without compromising the quality of the visual representation.

## 4 Experiments

We first show the empirical performance of our approach when applied to LLaVA-1.5 in Sec 4.1. We then demonstrate the effectiveness of each component in our model in Sec 4.3.

Table 1: Comparison with large multimodal models on six benchmarks. Our proposed approach LLaVA-PruMerge can adaptively reduce visual tokens, which uses only 5.5% visual tokens on average (on 6 tasks) and achieves competitive performance compared to the original LLaVA-1.5.

Method	LLM	Res.	PT	IT	VQA <sup>v2</sup>	SQA <sup>I</sup>	VQA <sup>T</sup>	POPE	MME	MMB
BLIP-2	Vicuna-13B	224	129M	-	41.0	61	42.5	85.3	1293.8	-
InstructBLIP	Vicuna-7B	224	129M	1.2M	-	60.5	50.1	-	-	36
InstructBLIP	Vicuna-13B	224	129M	1.2M	-	63.1	50.7	78.9	1212.8	-
Shikra	Vicuna-13B	224	600K	5.5M	77.4	-	-	-	-	58.8
IDEFICS-9B	LLaMA-7B	224	353M	1M	50.9	-	25.9	-	-	48.2
IDEFICS-80B	LLaMA-65B	224	353M	1M	60.0	-	30.9	-	-	54.5
Qwen-VL	Qwen-7B	448	1.4B	50M	78.8	67.1	63.8	-	-	38.2
Qwen-VL-Chat	Qwen-7B	448	1.4B	50M	78.2	68.2	61.5	-	1487.5	60.6
LLaVA-1.5	Vicuna-7B	336	558K	665K	78.5	66.8	58.2	85.9	1510.7	64.3
LLaVA-1.5 + Ours	Vicuna-7B	336	558K	665K	72.0	68.5	56.0	86.3	1350.3	60.9
LLaVA-1.5	Vicuna-13B	336	558K	665K	80.0	71.6	61.3	85.9	1531.3	67.7
LLaVA-1.5 + Ours	Vicuna-13B	336	558K	665K	72.8	71.0	58.4	86.2	1428.2	62.3

#### 4.1 Main Results

We apply our method to LLaVA-1.5 [Liu et al., 2023a], a recent state-of-the-art LMM. We further finetune LLaVA-1.5 using LoRA [Hu et al., 2022] for 1 epoch using the LLaVA-1.5 instruction fine-tuning data [Liu et al., 2023a] with our reduced visual tokens.

We evaluate on diverse visual question-answering and reasoning benchmarks including VQAv2 [Goyal et al., 2017], ScienceQA [Lu et al., 2022], TextVQA [Singh et al., 2019], POPE hallucination bench [Li et al., 2023b], MME [Fu et al., 2023], and MMBench [Liu et al., 2023c]. As shown in Table 1, our approach achieves comparable performance with LLaVA-1.5 while performing better than previous works such as BLIP2 [Li et al., 2023a] and InstructBLIP [Dai et al., 2023]. Specifically, in POPE and ScienceQA, our approach even shows better performance than LLaVA-1.5. Note that due to the adaptive nature of PruMerge (see Sec. 3.2), the token numbers for various tasks are different (see 4.3.1), and thus we use the average number on numbers of 6 tasks (*i.e.*, 32) for simplicity.

#### 4.2 Efficiency Analysis

Table 2: Computation Cost Analysis. The development device is TESLA V100 GPU, and time estimated by the roofline model represents the theoretical performance that the hardware can achieve.

Method	LLM Backbone	Quantization	FLOPs (T)	Prefill Time (ms)	Total Memory (G)	Storing Activation (G)
LLaVA-1.5	Vicuna-7B	FP16	9.3	88.6	23.3	4.60
LLaVA-1.5 w/ PruMerge	Vicuna-7B	FP16	0.91	15.3	13.7	0.28
LLaVA-1.5	Vicuna-7B	INT4	2.3	151.6	5.9	1.20
LLaVA-1.5 w/ PruMerge	Vicuna-7B	INT4	0.28	14.9	3.5	0.07
LLaVA-1.5	Vicuna-13B	FP16	18.2	170.5	41.6	7.30
LLaVA-1.5 w/ PruMerge	Vicuna-13B	FP16	1.80	29.5	26.6	0.44
LLaVA-1.5	Vicuna-13B	INT4	4.6	294.9	10.5	1.80
LLaVA-1.5 w/ PruMerge	Vicuna-13B	INT4	0.45	29.0	6.8	0.11

To elucidate the computational efficiency afforded by PruMerge, we utilize the roofline-based LLM-Viewer analysis as developed in [Yuan et al., 2024]. Our investigation is grounded in a theoretical scenario tailored to highlight the impact of PruMerge on processing efficiency within LMMs. Consider a typical scenario where an image of dimensions  $336 \times 336$  pixels is processed using a CLIP-ViT model, resulting in 576 visual tokens. Accompanying this image is a text prompt, assumed to contain 40 tokens for the sake of this analysis. Through the application of PruMerge, we achieve a dramatic reduction in the number of visual tokens, decreasing the original count by approximately 14.4 times in MME/TextVQA to match the token count of the text prompt ( $576/14.4 \approx 40$ ). The implications of this reduction are significant, as demonstrated in Table 2, which outlines the computational cost associated with the LMM prefill process. Notably, PruMerge not only enhances the speed of the LLM prefill process by reducing the required floating-point operations (FLOPs) but also contributes to a reduction in computational memory demands.

It is important to emphasize that the benefits of PruMerge extend beyond mere efficiency gains. Our token reduction strategy can complement other LLM acceleration techniques, such as quantization and factorization [Yuan et al., 2023b]. This orthogonal relationship underscores the versatile potential of PruMerge to contribute to a broader spectrum of efficiency-enhancing strategies.

### 4.3 Ablation Study

#### 4.3.1 Token Sampling Strategy Analysis

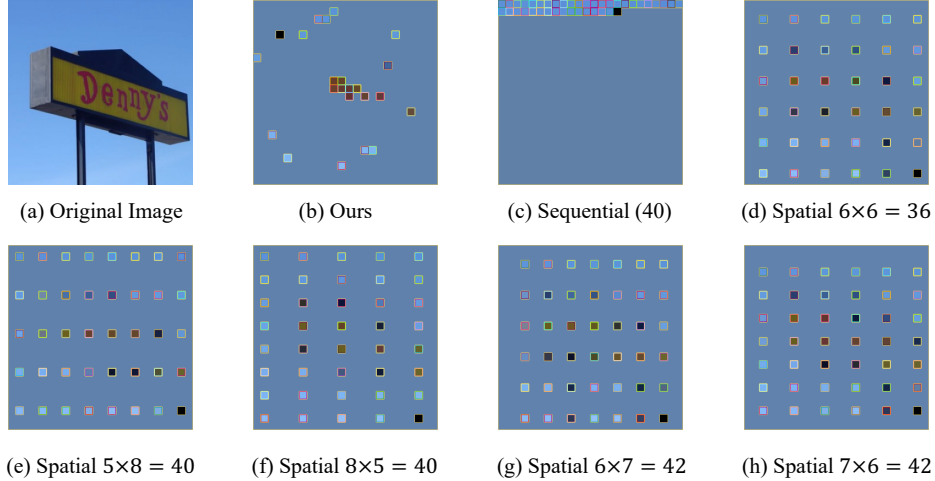


Figure 4: The demo of the different visual tokens sampling strategies.

Here we show how our approach performs better than the vanilla visual token sampling strategy, including sequential sampling and spatial sampling.

**LLaVA-PruMerge:** Our approach dynamically samples key visual tokens (see Sec. 3.2), which results in 40 visual tokens per image on average for TextVQA/MME, 35 tokens for POPE, and 16 tokens for SQA. The visualization is shown in Figure 4 (b).

**Sequential sampling:** We sample  $N$  tokens in the flattened visual tokens. For example, the first 40 tokens are sampled for an apple-to-apple comparison, shown in Figure 4 (c).

**Spatial sampling:** The sampled  $N$  tokens are evenly distributed across the image, as shown in Figure 4 (d-h). We study diverse settings, including  $6 \times 6$  (36 tokens),  $5 \times 8$  (40 tokens),  $8 \times 5$  (40 tokens),  $6 \times 7$  (42 tokens),  $7 \times 6$  (42 tokens),  $5 \times 7$  (35 tokens),  $7 \times 5$  (35 tokens), and  $4 \times 4$  (16 tokens), .

Note that all the experiments are done via the training-free manner. As shown in Table 3, our approach is consistently better than sequential sampling and spatial sampling across all downstream tasks, which demonstrates the effectiveness of the sampling mechanism of LLaVA-PruMerge. Importantly, we observe that LLaVA-PruMerge shows much better performance on TextVQA [Singh et al., 2019]. Such Optical Character Recognition (OCR) task requires detailed information about the text, which demonstrates that LLaVA-PruMerge extracts the key information in the images with enough details. This quantitative result aligns with the visualization

Table 3: Token Sampling Strategy Analysis on Different Tasks. Due to the fact that PruMerge can choose the number of visual tokens based on the input image information density, the number of tokens used in different tasks may differ.

Approach	#Visual Tokens	Performance
Task: VQA <sup>†</sup>		
LLaVA-PruMerge	40	54.00
Sequential	40	42.72
Spatial	$6 \times 6 = 36$	46.84
	$5 \times 8 = 40$	46.85
	$8 \times 5 = 40$	47.42
	$6 \times 7 = 42$	47.96
	$7 \times 6 = 42$	47.49
Task: MME		
LLaVA-PruMerge	40	1250.07
Sequential	40	703.60
Spatial	$6 \times 6 = 36$	1169.10
	$5 \times 8 = 40$	1180.23
	$8 \times 5 = 40$	1142.32
	$6 \times 7 = 42$	1220.89
	$7 \times 6 = 42$	1199.10
Task: POPE		
LLaVA-PruMerge	35	76.2
Sequential	35	11.7
Spatial	$5 \times 7 = 35$	69.8
	$7 \times 5 = 35$	71.1
	$6 \times 6 = 36$	67.9
Task: SQA <sup>‡</sup>		
LLaVA-PruMerge	16	68.07
Sequential	16	64.20
Spatial	$4 \times 4 = 16$	66.29



of LLaVA-PruMerge attentive tokens in Figure 1a (b), where more attentive tokens are distributed on the foreground text in the images.

#### 4.3.2 Effectiveness of Each Module in PruMerge

Table 4: Ablation Studies for Adaptive Important Token Selection (AITS, Sec. 3.2) and Token Supplement (TS, Sec. 3.3). With these modules, the downstream performance can be progressively improved.

Method	LLM	SQA <sup>I</sup>	VQA <sup>T</sup>	POPE	MME
LLaVA-1.5	Vicuna-7B	66.8	58.2	85.9	1510.7
LLaVA-1.5 w/ AITS	Vicuna-7B	66.5	54.8	85.7	1221.6
LLaVA-1.5 w/ AITS & TS	Vicuna-7B	68.5	56.0	86.3	1350.3

Here, we study the effectiveness of each module in our design based on LLaVA-1.5. Note that we maintain the same amount of visual tokens (6.9%, 40 tokens) across all settings. As shown in Table 4, after progressively adding the proposed modules, including Adaptive Important Token Selection (AITS) and Token Supplement (TS), the downstream performance can be further enhanced.

#### 4.3.3 Training Analysis: Training-free v.s. Fine-tuning

LLaVA-PruMerge can be conducted both in training-free and training-needed manners. With fine-tuning, the large language model can adapt to the new structure of visual tokens, which could further enhance the performance on vision-language tasks. As shown in Table 5, with fine-tuning, our approach does bring better performance for diverse tasks, including ScienceQA [Lu et al., 2022], TextVQA [Singh et al., 2019], POPE [Li et al., 2023b], and MME [Fu et al., 2023].

Table 5: Ablation on training free and fine-tuning for our approach. With further fine-tuning, the performance of LLaVA-PruMerge can be further enhanced.

Method	LLM	SQA <sup>I</sup>	VQA <sup>T</sup>	POPE	MME
LLaVA-1.5	Vicuna-7B	66.8	58.2	85.9	1510.7
LLaVA-PruMerge w.o. fine-tuning	Vicuna-7B	68.0	54.0	76.2	1250.1
LLaVA-PruMerge w. fine-tuning	Vicuna-7B	68.5	56.0	86.3	1350.3

## 5 Conclusion

In this paper, we improve the efficiency of Large Multimodal Models (LMMs) from the perspective of reducing the quantity of visual tokens. By leveraging the spatial redundancy in visual tokens, we proposed a plug-and-play token reduction module that employs the similarity between the class token and spatial tokens as a key criterion for pruning and merging visual tokens.

Our approach, applied to LLaVA-1.5, demonstrated that by utilizing only 6.9% of visual tokens on average, the pruned tokens can maintain comparable performance across a wide range of visual question-answering and reasoning tasks. Notably, our work highlights the potential for significant computational savings without sacrificing the reasoning capabilities of LMMs. We hope our work inspires further exploration into the interplay between efficiency and performance in LMMs.

## 6 Limitations and Future Work

Our exploration of LLaVA-PruMerge has two primary limitations. First, the visual token compression, while efficient, is not entirely lossless. This results in a marginal performance gap between the original model (LLaVA) and our optimized version LLaVA-PruMerge. We are committed to advancing our research towards achieving a fully lossless token compression algorithm, aiming to close these performance gaps. Second, the scope of our validation efforts is somewhat constrained

by the computational resources typically available in academic settings. This limitation has precluded a comprehensive assessment of PruMerge’s applicability to larger-scale models, such as those envisioned in the LLaVA-Next [Liu et al., 2023a] framework with a Yi-34B backbone. Future investigations will seek to extend our methodology to these more expansive model architectures, exploring its potential for generalization and broader impact.

## **Acknowledgement**

This work was supported in part by NSF CAREER IIS2150012, and Institute of Information & communications Technology Planning & Evaluation(IITP) grants funded by the Korea government(MSIT) (No. 2022-0-00871, Development of AI Autonomy and Knowledge Enhancement for AI Agent Collaboration) and (No. RS2022-00187238, Development of Large Korean Language Model Technology for Efficient Pre-training), and Microsoft Accelerate Foundation Models Research Program.

## References

- Jean-Baptiste Alayrac, Jeff Donahue, Pauline Luc, Antoine Miech, Iain Barr, Yana Hasson, Karel Lenc, Arthur Mensch, Katherine Millican, Malcolm Reynolds, et al. Flamingo: a visual language model for few-shot learning. *NeurIPS*, 35:23716–23736, 2022.
- Jimmy Lei Ba, Jamie Ryan Kiros, and Geoffrey E Hinton. Layer normalization. *arXiv preprint arXiv:1607.06450*, 2016.
- Daniel Bolya, Cheng-Yang Fu, Xiaoliang Dai, Peizhao Zhang, Christoph Feichtenhofer, and Judy Hoffman. Token merging: Your ViT but faster. In *International Conference on Learning Representations*, 2023.
- Azzedine Boukerche, Lining Zheng, and Omar Alfandi. Outlier detection: Methods, models, and classification. *ACM Computing Surveys (CSUR)*, 2020.
- Mu Cai, Haotian Liu, Siva Karthik Mustikovela, Gregory P. Meyer, Yuning Chai, Dennis Park, and Yong Jae Lee. Making large multimodal models understand arbitrary visual prompts. In *IEEE Conference on Computer Vision and Pattern Recognition*, 2024.
- Keqin Chen, Zhao Zhang, Weili Zeng, Richong Zhang, Feng Zhu, and Rui Zhao. Shikra: Unleashing multimodal llm’s referential dialogue magic. *arXiv preprint arXiv:2306.15195*, 2023.
- Xiangxiang Chu, Limeng Qiao, Xinyang Lin, Shuang Xu, Yang Yang, Yiming Hu, Fei Wei, Xinyu Zhang, Bo Zhang, Xiaolin Wei, et al. Mobilevlm: A fast, reproducible and strong vision language assistant for mobile devices. *arXiv preprint arXiv:2312.16886*, 2023.
- Xiangxiang Chu, Limeng Qiao, Xinyu Zhang, Shuang Xu, Fei Wei, Yang Yang, Xiaofei Sun, Yiming Hu, Xinyang Lin, Bo Zhang, et al. Mobilevlm v2: Faster and stronger baseline for vision language model. *arXiv preprint arXiv:2402.03766*, 2024.
- Wenliang Dai, Junnan Li, Dongxu Li, Anthony Meng Huat Tiong, Junqi Zhao, Weisheng Wang, Boyang Li, Pascale Fung, and Steven Hoi. Instructblip: Towards general-purpose vision-language models with instruction tuning, 2023.
- Tim Dettmers, Mike Lewis, Younes Belkada, and Luke Zettlemoyer. Gpt3. int8 (): 8-bit matrix multiplication for transformers at scale. *Advances in Neural Information Processing Systems*, 35:30318–30332, 2022.
- Alexey Dosovitskiy, Lucas Beyer, Alexander Kolesnikov, Dirk Weissenborn, Xiaohua Zhai, Thomas Unterthiner, Mostafa Dehghani, Matthias Minderer, Georg Heigold, Sylvain Gelly, et al. An image is worth 16x16 words: Transformers for image recognition at scale. *arXiv preprint arXiv:2010.11929*, 2020.
- Chaoyou Fu, Peixian Chen, Yunhang Shen, Yulei Qin, Mengdan Zhang, Xu Lin, Zhenyu Qiu, Wei Lin, Jinrui Yang, Xiawu Zheng, et al. Mme: A comprehensive evaluation benchmark for multimodal large language models. *arXiv preprint arXiv:2306.13394*, 2023.
- Yash Goyal, Tejas Khot, Douglas Summers-Stay, Dhruv Batra, and Devi Parikh. Making the v in vqa matter: Elevating the role of image understanding in visual question answering. In *Proceedings of the IEEE conference on computer vision and pattern recognition*, pp. 6904–6913, 2017.
- Kai Han, Yunhe Wang, Hanqing Chen, Xinghao Chen, Jianyuan Guo, Zhenhua Liu, Yehui Tang, An Xiao, Chunjing Xu, Yixing Xu, et al. A survey on vision transformer. *TPAMI*, 2022.
- Dan Hendrycks and Kevin Gimpel. Gaussian error linear units (gelus). *arXiv preprint arXiv:1606.08415*, 2016.
- Yining Hong, Haoyu Zhen, Peihao Chen, Shuhong Zheng, Yilun Du, Zhenfang Chen, and Chuang Gan. 3d-llm: Injecting the 3d world into large language models. *NeurIPS*, 2023.
- Edward J Hu, Yelong Shen, Phillip Wallis, Zeyuan Allen-Zhu, Yuanzhi Li, Shean Wang, Lu Wang, and Weizhu Chen. LoRA: Low-rank adaptation of large language models. In *International Conference on Learning Representations*, 2022. URL <https://openreview.net/forum?id=nZeVKeeFYf9>.
- Mojan Javaheripi, Sébastien Bubeck, Marah Abdin, Jyoti Aneja, Sebastien Bubeck, Caio César Teodoro Mendes, Weizhu Chen, Allie Del Giorno, Ronen Eldan, Sivakanth Gopi, et al. Phi-2: The surprising power of small language models. *Microsoft Research Blog*, 2023.
- Albert Q Jiang, Alexandre Sablayrolles, Arthur Mensch, Chris Bamford, Devendra Singh Chaplot, Diego de las Casas, Florian Bressand, Gianna Lengyel, Guillaume Lample, Lucile Saulnier, et al. Mistral 7b. *arXiv preprint arXiv:2310.06825*, 2023.

- Nikita Kitaev, Lukasz Kaiser, and Anselm Levskaya. Reformer: The efficient transformer. In *International Conference on Learning Representations*, 2020. URL <https://openreview.net/forum?id=rkgNKkHtvB>.
- Junnan Li, Dongxu Li, Silvio Savarese, and Steven C. H. Hoi. Blip-2: Bootstrapping language-image pre-training with frozen image encoders and large language models. In *International Conference on Machine Learning*, 2023a. URL <https://api.semanticscholar.org/CorpusID:256390509>.
- Yifan Li, Yifan Du, Kun Zhou, Jinpeng Wang, Wayne Xin Zhao, and Ji-Rong Wen. Evaluating object hallucination in large vision-language models. *arXiv preprint arXiv:2305.10355*, 2023b.
- Youwei Liang, Chongjian Ge, Zhan Tong, Yibing Song, Jue Wang, and Pengtao Xie. Not all patches are what you need: Expediting vision transformers via token reorganizations. *arXiv preprint arXiv:2202.07800*, 2022.
- Bin Lin, Bin Zhu, Yang Ye, Munan Ning, Peng Jin, and Li Yuan. Video-llava: Learning united visual representation by alignment before projection. *arXiv preprint arXiv:2311.10122*, 2023.
- Bin Lin, Zhenyu Tang, Yang Ye, Jiaxi Cui, Bin Zhu, Peng Jin, Junwu Zhang, Munan Ning, and Li Yuan. Moe-llava: Mixture of experts for large vision-language models. *arXiv preprint arXiv:2401.15947*, 2024.
- Haotian Liu, Chunyuan Li, Yuheng Li, and Yong Jae Lee. Improved baselines with visual instruction tuning, 2023a.
- Haotian Liu, Chunyuan Li, Qingyang Wu, and Yong Jae Lee. Visual instruction tuning. *arXiv:2304.08485*, 2023b.
- Haotian Liu, Chunyuan Li, Yuheng Li, Bo Li, Yuanhan Zhang, Sheng Shen, and Yong Jae Lee. Llava-next: Improved reasoning, ocr, and world knowledge. 2024.
- Xiangcheng Liu, Tianyi Wu, and Guodong Guo. Adaptive sparse vit: Towards learnable adaptive token pruning by fully exploiting self-attention. *arXiv preprint arXiv:2209.13802*, 2022.
- Yuan Liu, Haodong Duan, Yuanhan Zhang, Bo Li, Songyang Zhang, Wangbo Zhao, Yike Yuan, Jiaqi Wang, Conghui He, Ziwei Liu, et al. Mmbench: Is your multi-modal model an all-around player? *arXiv preprint arXiv:2307.06281*, 2023c.
- Pan Lu, Swaroop Mishra, Tanglin Xia, Liang Qiu, Kai-Wei Chang, Song-Chun Zhu, Oyvind Tafjord, Peter Clark, and Ashwin Kalyan. Learn to explain: Multimodal reasoning via thought chains for science question answering. *Advances in Neural Information Processing Systems*, 2022.
- OpenAI. Gpt-4v(ision) system card. [https://cdn.openai.com/papers/GPTV\\_System\\_Card.pdf](https://cdn.openai.com/papers/GPTV_System_Card.pdf), 2023a.
- OpenAI. Gpt-4 technical report. 2023b.
- Zhiliang Peng, Wenhui Wang, Li Dong, Yaru Hao, Shaohan Huang, Shuming Ma, and Furu Wei. Kosmos-2: Grounding multimodal large language models to the world. *arXiv preprint arXiv:2306.14824*, 2023.
- Alec Radford, Jong Wook Kim, Chris Hallacy, Aditya Ramesh, Gabriel Goh, Sandhini Agarwal, Girish Sastry, Amanda Askell, Pamela Mishkin, Jack Clark, et al. Learning transferable visual models from natural language supervision. In *International conference on machine learning*, pp. 8748–8763. PMLR, 2021.
- Yuzhang Shang, Zhihang Yuan, and Zhen Dong. Pb-llm: Partially binarized large language models. In *ICLR*, 2024.
- Amanpreet Singh, Vivek Natarajan, Meet Shah, Yu Jiang, Xinlei Chen, Dhruv Batra, Devi Parikh, and Marcus Rohrbach. Towards vqa models that can read. In *Proceedings of the IEEE/CVF conference on computer vision and pattern recognition*, pp. 8317–8326, 2019.
- Yi Tay, Mostafa Dehghani, Dara Bahri, and Donald Metzler. Efficient transformers: A survey. *ACM Computing Surveys*, 2022.
- Gemini Team, Rohan Anil, Sebastian Borgeaud, Yonghui Wu, Jean-Baptiste Alayrac, Jiahui Yu, Radu Soricut, Johan Schalkwyk, Andrew M Dai, Anja Hauth, et al. Gemini: a family of highly capable multimodal models. *arXiv preprint arXiv:2312.11805*, 2023.
- Hugo Touvron, Thibaut Lavril, Gautier Izacard, Xavier Martinet, Marie-Anne Lachaux, Timothée Lacroix, Baptiste Rozière, Naman Goyal, Eric Hambro, Faisal Azhar, et al. Llama: Open and efficient foundation language models. *arXiv preprint arXiv:2302.13971*, 2023.

- Ashish Vaswani, Noam Shazeer, Niki Parmar, Jakob Uszkoreit, Llion Jones, Aidan N Gomez, Łukasz Kaiser, and Illia Polosukhin. Attention is all you need. In *Advances in Neural Information Processing Systems*, pp. 5998–6008, 2017.
- Vicuna. Vicuna: An open-source chatbot impressing gpt-4 with 90%\* chatgpt quality. <https://vicuna.lmsys.org/>, 2023.
- Sinong Wang, Belinda Z. Li, Madian Khabsa, Han Fang, and Hao Ma. Linformer: Self-attention with linear complexity, 2020.
- Haoran Wei, Lingyu Kong, Jinyue Chen, Liang Zhao, Zheng Ge, En Yu, Jianjian Sun, Chunrui Han, and Xiangyu Zhang. Small language model meets with reinforced vision vocabulary. *arXiv preprint arXiv:2401.12503*, 2024.
- Hongxu Yin, Arash Vahdat, Jose M Alvarez, Arun Mallya, Jan Kautz, and Pavlo Molchanov. A-vit: Adaptive tokens for efficient vision transformer. In *Proceedings of the IEEE/CVF Conference on Computer Vision and Pattern Recognition*, pp. 10809–10818, 2022.
- Shukang Yin, Chaoyou Fu, Sirui Zhao, Ke Li, Xing Sun, Tong Xu, and Enhong Chen. A survey on multimodal large language models. *arXiv preprint arXiv:2306.13549*, 2023.
- Zhengqing Yuan, Zhaoxu Li, and Lichao Sun. Tinygpt-v: Efficient multimodal large language model via small backbones. *arXiv preprint arXiv:2312.16862*, 2023a.
- Zhihang Yuan, Yuzhang Shang, Yue Song, Qiang Wu, Yan Yan, and Guangyu Sun. Asvd: Activation-aware singular value decomposition for compressing large language models. *arXiv preprint arXiv:2312.05821*, 2023b.
- Zhihang Yuan, Yuzhang Shang, Yang Zhou, Zhen Dong, Chenhao Xue, Bingzhe Wu, Zhikai Li, Qingyi Gu, Yong Jae Lee, Yan Yan, et al. Llm inference unveiled: Survey and roofline model insights. *arXiv preprint arXiv:2402.16363*, 2024.
- Duzhen Zhang, Yahan Yu, Chenxing Li, Jiahua Dong, Dan Su, Chenhui Chu, and Dong Yu. Mm-llms: Recent advances in multimodal large language models. *arXiv preprint arXiv:2401.13601*, 2024.
- Hang Zhang, Xin Li, and Lidong Bing. Video-llama: An instruction-tuned audio-visual language model for video understanding. *arXiv preprint arXiv:2306.02858*, 2023a.
- Shilong Zhang, Peize Sun, Shoufa Chen, Min Xiao, Wenqi Shao, Wenwei Zhang, Kai Chen, and Ping Luo. Gpt4roi: Instruction tuning large language model on region-of-interest. *arXiv preprint arXiv:2307.03601*, 2023b.
- Baichuan Zhou, Ying Hu, Xi Weng, Junlong Jia, Jie Luo, Xien Liu, Ji Wu, and Lei Huang. Tinyllava: A framework of small-scale large multimodal models. *arXiv preprint arXiv:2402.14289*, 2024.
- Deyao Zhu, Jun Chen, Xiaoqian Shen, Xiang Li, and Mohamed Elhoseiny. Minigpt-4: Enhancing vision-language understanding with advanced large language models. *arXiv preprint arXiv:2304.10592*, 2023.
- Yichen Zhu, Minjie Zhu, Ning Liu, Zhicai Ou, Xiaofeng Mou, and Jian Tang. Llava-phi: Efficient multi-modal assistant with small language model. *arXiv preprint arXiv:2401.02330*, 2024.